Microstrip/Slotline Transitions: Modeling and Experimental Investigation

BERND SCHÜPPERT

Abstract—**In this paper an analysis of microstrip/slotline transitions is given using a network description through transmission-line models. Different transitions, such as transitions containing uniform and nonuniform lines as well as soldered and virtually shorted microstrip lines, will be treated. The validity of the modeling results is verified experimentally by measuring the transmission coefficient of a cascade of two transitions separated by a slotline in the frequency range from 1 to 16 GHz. For practical applications, design curves are given for 0.635-mm-thick alumina substrates.**

I. Introduction

MANY AUTHORS have dealt with the problem of developing a broad-band transition from microstrip to slotline [1]–[6]. Some intuitive approaches to this problem have been presented with a reported bandwidth between about 1 octave [1] and 1 decade [3], the latter in the frequency range from 1 to 10 GHz.

A problem quite similar to the subject considered here has been treated in [7], where a nonplanar compensated balun has been presented for frequencies below 1 GHz. However, some basic results are similar to those given here. Due to the fact that a systematical description of this problem is still lacking, the present paper is intended to give an approach to this problem based on the use of transmission-line models. In the case of circular-area stubs, these lines will be synthesized as piecewise uniform lines. The validity of this rough approximation will be verified by experimental results.

The transitions mentioned in this paper are sketched in Fig. 1. Concerning experimental verification, the question of how to measure the frequency response of a single transition arises. A measurement of only the *VSWR* or reflection coefficient at the microstrip side when the slotline is matched [2], [4]–[6] ignores matching through radiation effects of the slot stub. Moreover, increasing line loss at higher frequencies also yields a low *VSWR* of the transition. Both effects suggest a bandwidth of the transition that may be too large.

When measuring the transmission and/or reflection coefficient of two transitions connected through a slotline of length L_s [3], [6], impedance interactions occur between the transitions. As a result, the measured bandwidth of such a configuration depends on the distance between the transitions, which is somewhat arbitrary.

Manuscript received October 30, 1987; revised March 16, 1988.

The author is with the Technische Universität Berlin, Institut für Hochfrequenztechnik, D-1000 Berlin 10, West Germany.

IEEE Log Number 8821761.

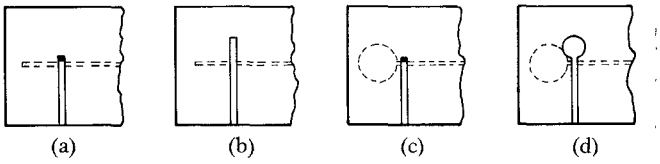

Fig. 1. Microstrip/slotline transitions under consideration; solid lines: microstrip circuitry; dashed lines: slotline circuitry. (a) Soldered microstrip short and uniform $\lambda/4$ slotline. (b) Virtual short with uniform $\lambda/4$ open microstrip and uniform $\lambda/4$ slotline. (c) Soldered microstrip short and slotline open circuit through nonuniform circular slotline. (d) Virtual short with nonuniform circular microstrip and slotline open circuit through nonuniform circular slotline.

II. Simplified Model for Circuit Analysis

In order to clarify the effects, let us first consider simplified circuit models. It will be shown that the transition of Fig. 1(b) offers either an improved flatness of the frequency response or an improved bandwidth by means of a reactance compensation effect [7] compared to the transition of Fig. 1(a). This reactance compensation effect also takes place in the case of nonuniform lines. However, if these lines are of a circular shape (Fig. 1(d)), only an improved flatness is observable, whereas the bandwidth is somewhat smaller than in the case of a soldered transition (Fig. 1(c)).

It should be pointed out that in the following approximations any reactances due to the discontinuities are neglected.

In the presence of uniform microstrip and slotlines, equivalent circuits for both of the transitions of Fig. 1(a) and (b) are shown in Fig. 2, where the soldered wire can be represented by a series inductance, which, however, will be neglected. Equivalent circuits as simple as those given in Fig. 2(a) and (b) imply that perfect coupling between the microstrip and slotline currents takes place.

If we choose the characteristic impedances of microstrip and slotline to be

$$Z_m = Z_s = 50\ \Omega \tag{1}$$

it is convenient to introduce normalized impedance factors for shorted slot stub and open microstrip stub, respectively:

$$v = \frac{Z_{ss}}{50\ \Omega} \tag{2}$$

$$w = \frac{50\ \Omega}{Z_{mo}}. \tag{3}$$

0018-9480/88/0800-1272$01.00 ©1988 IEEE

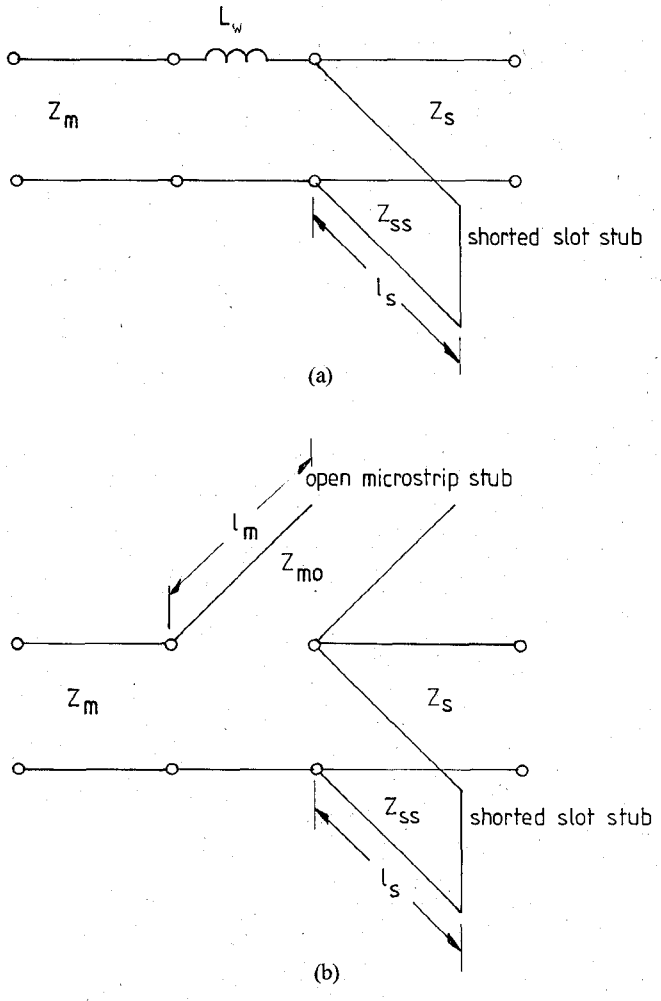

Fig. 2. Simplified equivalent circuits of a microstrip/slotline transition. (a) with soldered wire. (b) with virtual short.

For simplification let us assume slotline stub and microstrip stub to have the same electrical length ($\beta_m l_m = \beta_s l_s = \beta l$).

Analyzing the transition of Fig. 1(a) (equivalent circuit Fig. 2(a)), the magnitude of the transmission coefficient becomes

$$|S_{21}| = \frac{1}{\sqrt{1 + \frac{1}{v^2}\frac{\cot^2 \beta l}{4}}}. \tag{4}$$

A -0.97 dB bandwidth can be defined when choosing

$$v = \cot \beta l \tag{5}$$

leading to a bandwidth value of

$$B = \frac{f_2|_{-0.97\,\mathrm{dB}}}{f_1|_{-0.97\,\mathrm{dB}}} = \frac{= \pi - \arctan \frac{1}{v}}{\arctan \frac{1}{v}} \tag{6}$$

which is plotted in Fig. 3. It should be noted that the -0.97 dB bandwidth of the insertion loss corresponds to a $VSWR = 2.6$, if the network is lossless.

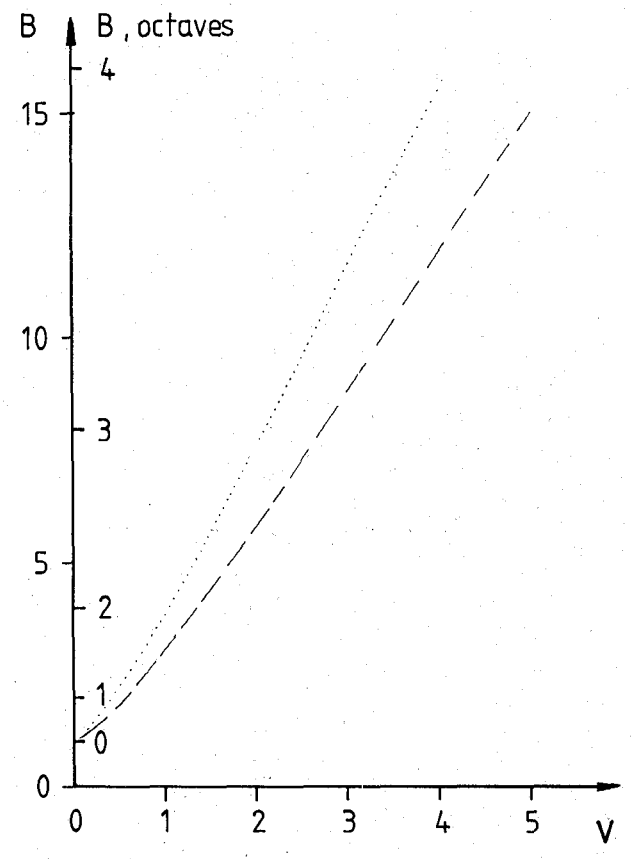

Fig. 3. -0.97 dB bandwidth against impedance factor v for a *single* transition. ----- soldered short and virtual short with $v = w$; ••••• virtual short, $w = 2.618v$ (optimum bandwidth).

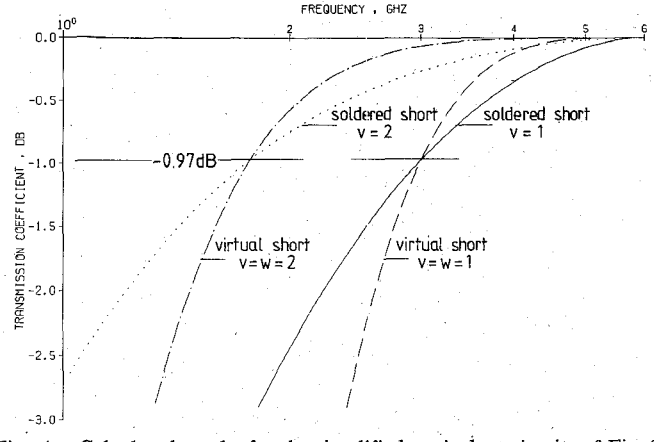

Fig. 4. Calculated results for the simplified equivalent circuits of Fig. 2 for a single transition using a *uniform* slotline stub, lower frequency range.

In the case of a virtual short (Figs. 1(b) and 2(b)) the magnitude of the transmission coefficient becomes

$$|S_{21}| = \frac{1}{\sqrt{1 + \underbrace{\left(\frac{1}{v} - \frac{1}{w}\right)^2 \frac{\cot^2 \beta l}{4}}_{\text{dominant in the passband}} + \underbrace{\frac{1}{(vw)^2}\frac{\cot^4 \beta l}{4}}_{\text{dominant at the band limits}}}} \tag{7}$$

TABLE I
INFLUENCE OF VARIOUS VIRTUAL SHORT CONDITIONS ON THE BANDWIDTH OF A SINGLE TRANSITION

	Impedance Factors	Bandwidth $B\|_{-0.97\,\mathrm{dB}}$	$\|S_{21}\|$ at $f_{-0.97\,\mathrm{dB}}$ of Soldered Short	Remarks
Soldered short	v	B_{soldered}	-0.97 dB	reference
Virtual short	$w=v$	B_{soldered}	-0.97 dB	maximal flat frequency response in the passband
Virtual short	$w=2v$	$B_{\mathrm{soldered}} < B < B_{\mathrm{opt}}$	$\|S_{21\,\mathrm{opt}}\| = -0.51$ dB	
Virtual short	$w=2.618v$	$B_{\mathrm{opt}} \approx 1.2\cdots1.3\cdot B_{\mathrm{soldered}}$	-0.51 dB $\cdots$ -0.97 dB	maximal -0.97 dB bandwidth
Virtual short	$w\to\infty$	B_{soldered}	-0.97 dB	like soldered short

and it is evident from the above equation that choosing $v=w$ yields a maximum flat frequency response in the passband.

In this case where $v=w$, the -0.97 dB bandwidth remains unchanged between soldered or virtual short, so (6), as well as the calculations of Fig. 3, is also valid when dealing with a virtual short!

To clarify the results discussed above, numerical calculations of the frequency response have been carried out for the equivalent circuits of Fig. 2(a) and (b). Due to the symmetry properties of the frequency response it is sufficient to calculate only the lower frequency range.

It can be seen from Fig. 4 that the bandwidth is improved with increasing $v=w$, as already predicted by Fig. 3 and [7]. The -0.97 dB bandwidth is the same in case of a soldered or a virtual short with $v=w$. Furthermore, an improved flatness of the frequency response in the passband is noticeable.

However, a more interesting case is that of an improved bandwidth by means of a virtual short. Considering (7), an extreme value of $|S_{21}|$ can be found through

$$\frac{d|S_{21}|}{dw}=0 \tag{8}$$

leading to a maximally flat frequency response if

$$w=v\left(1+\frac{\cot^2\beta l}{v^2}\right) \tag{9}$$

and an optimum value of

$$|S_{21}|=\frac{1}{\sqrt{1+\dfrac{1}{4v^2}\dfrac{\cot^4\beta l}{v^2+\cot^2\beta l}}}. \tag{10}$$

Considering the -0.97 dB frequencies of a soldered short, which are given through (5), an optimal relation between both impedance factors can be deduced by inserting (5) in (9), yielding

$$w=2v. \tag{11}$$

In this case, the transmission coefficient $|S_{21}|$ at the -0.97 dB frequencies of a soldered short is increased optimally at a value of $|S_{21}|=-0.51$ dB. If we consider the maximum achievable -0.97 dB bandwidth of the optimal case described by (10), we get an optimal relation between both impedance factors:

$$w=2.618v \tag{12}$$

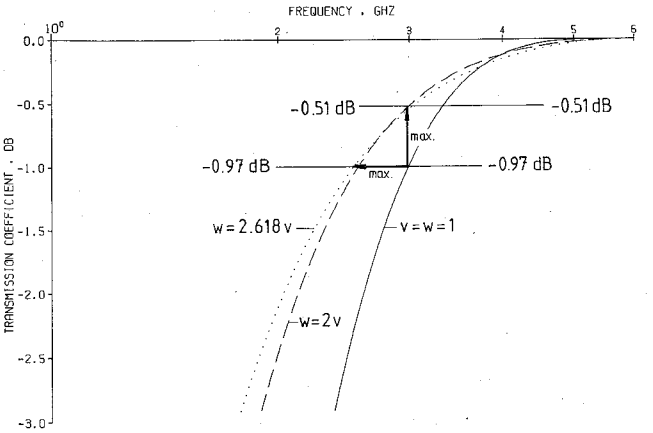

Fig. 5. Calculated results for the simplified equivalent circuit of Fig. 2 for a single transition with *uniform* stubs, lower frequency range.

and a bandwidth of

$$B=\frac{f_2|_{-0.97\,\mathrm{dB}}}{f_1|_{-0.97\,\mathrm{dB}}}=\frac{\pi-\arctan\dfrac{1}{1.272v}}{\arctan\dfrac{1}{1.272v}} \tag{13}$$

as sketched in Fig. 3 (dotted line), yielding an optimally increased bandwidth compared to the soldered short of (5) of approximately

$$B_{\mathrm{virtual}}\approx(1.2\cdots1.3)\,B_{\mathrm{soldered}}. \tag{14}$$

Summarizing this section, a comparison between soldered and virtual short is given in Table I and depicted in Fig. 5.

III. TRANSITIONS WITH UNIFORM MICROSTRIP AND SLOTLINES

This section is intended to verify the results of Section II experimentally. For practical applications, these transitions offer a smaller bandwidth compared to transitions incorporating nonuniform stubs, which will be treated in Section IV.

A transition with uniform lines has been treated in [6] using an equivalent circuit which is quite similar to that given in Fig. 2(b), yielding a bandwidth of 1.45 octaves in the frequency range from 2.6 to 7.1 GHz, if a $VSWR \leqslant 1.5$ is accepted for two transitions in cascade.

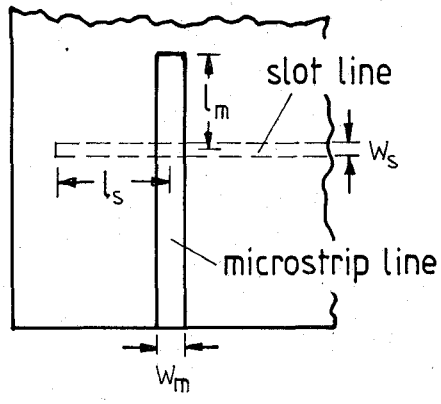

Fig. 6. Microstrip/slotline transition with uniform stubs.

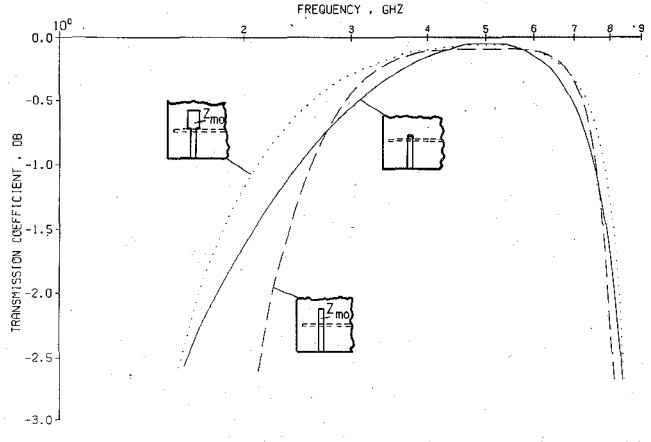

Fig. 7. *Calculated* transmission coefficient of a *single* microstrip/slotline transition with *uniform* stubs. —— soldered microstrip short; ----- virtual microstrip short, $Z_{mo} = 50\ \Omega$; ••••• virtual microstrip short, $Z_{mo} = 19\ \Omega$.

A. Single Transitions

The transitions considered here are sketched in Fig. 2(a) and (b), respectively. A more detailed view of a transition is given in Fig. 6. The dimensions are chosen for a center frequency of about 5.0 GHz and an alumina substrate with $\epsilon_r = 9.7$ and a thickness of $h = 0.635$ mm. Using the formulas given in [8], the following microstrip dimensions were used: microstrip width $w_m = 0.57$ mm and microstrip stub length (in case of a virtual short) $l_m = 5.7$ mm. The slotline characteristics have been calculated with a computer program referring to [9]. The dimensions are slotline width $w_s = 0.05$ mm (yielding a characteristic impedance which slightly exceeds the value of 50 Ω) and a slot stub length of $l_s = 7.3$ mm.

In the case of a soldered short, a 0.57-mm-wide copper sheet is fed through the substrate and soldered at both sides.

The calculated results for both virtual and soldered microstrip shorts are given in Fig. 7. The −0.97 dB bandwidth is approximately the same in both cases, consistent with the results of Section II, if both impedance factors are equal ($w = v$). The small differences between the upper and lower −0.97 dB frequency limits in the case of soldered and virtual shorts are due to slotline dispersion. The achievable −0.97 dB bandwidth is about 1.7 octaves.

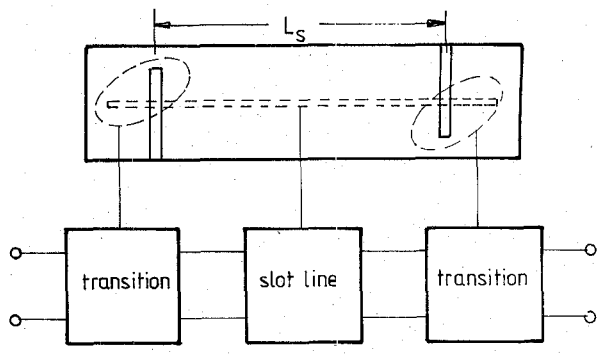

Fig. 8. Cascade of two transitions, separated by a slotline.

This bandwidth can easily be increased if we remember that an impedance relation of $w = 2.618v$ (eq. (12)) offers an optimum −0.97 dB bandwidth. For this, a characteristic impedance of about 19 Ω is necessary for the open-ended microstrip stub, which corresponds to a microstrip stub width of 3.0 mm. Due to the changed dispersion characteristics, the microstrip stub length is chosen to be $l_m = 5.2$ mm. The results are also given in Fig. 7 and it can be seen that the −0.97 dB bandwidth is increased to a value of about 1.9 octaves by simply broadening the microstrip stub.

B. Experimental Verification

The measurement setup is an automatic network analyzer (HP 8410 series) working in the frequency range from 1 to 18 GHz. However, full accuracy is only available from 2 to 12 GHz with this setup. Using the well-known calibration techniques, the network analyzer system errors are compensated. If these calibrations are carried out on the microstrip line, the transitions between coaxial and microstrip line can be compensated, too. However, at higher frequencies—above 12 GHz (see Section IV)—a residual error is still observable yielding an increased scattering of the measured data.

As mentioned above, the question arises how to measure the frequency response of a single transition. The simplest but not the most sensitive way is to measure the transmission coefficient of a cascade of two transitions separated by a slotline, as sketched in Fig. 8.

In order to show the influence of the length of the separating slotline, calculations have been carried out for transitions separated by two different slotline lengths ($L_s = 15$ mm and $L_s = 30$ mm). The modeling and experimental results are presented in Fig. 9(a) and (b). It is recognizable that the influence of the slotline length on the frequency response is significant.

Good agreement has been obtained between modeling and experiment in both cases. Due to transformation effects from one transition to the other, the ripple of the transmission coefficient at the band limits increases with increasing slotline length, both theoretically and experimentally.

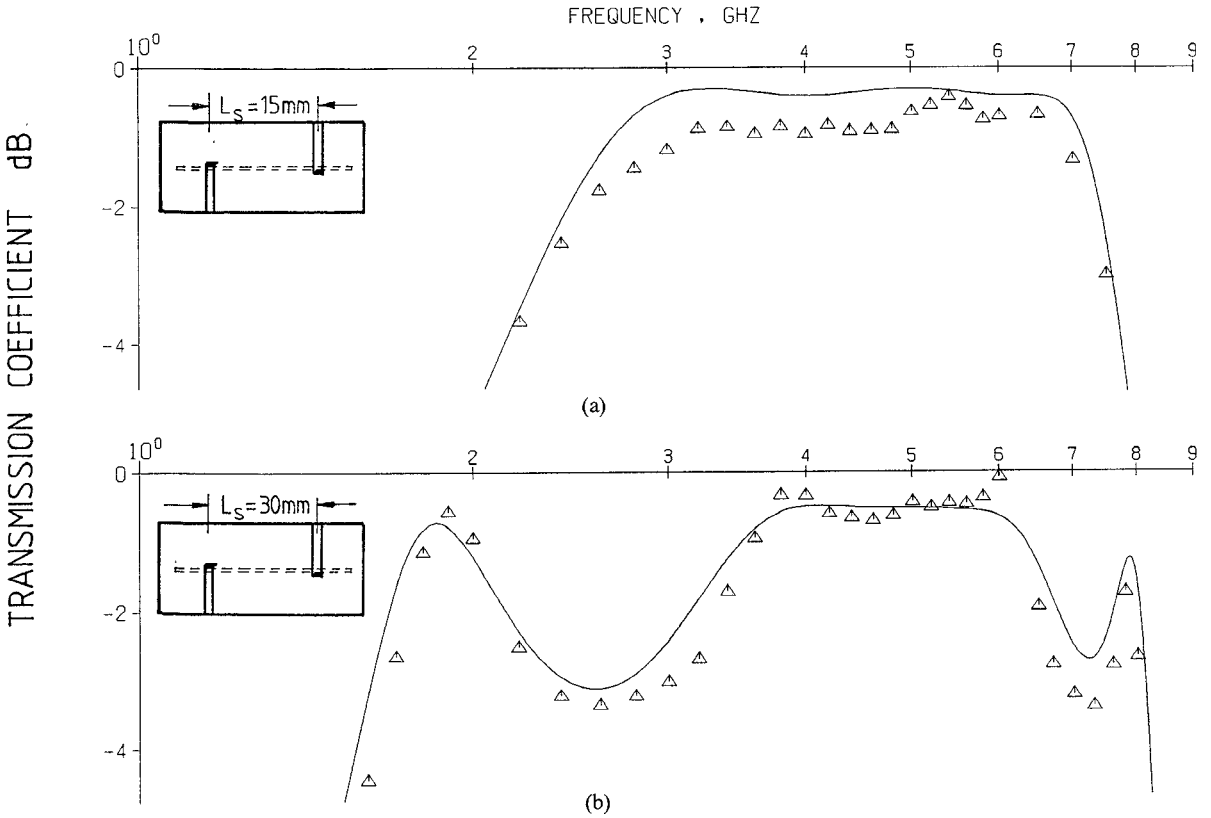

Fig. 9. Transmission coefficient of a cascade of two microstrip/slotlines transitions with a soldered microstrip short and *uniform* slotline stub, separated by slotlines of different length. Theoretical (——) and experimental (△) results. (a) $L_s = 15$ mm. (b) $L_s = 30$ mm.

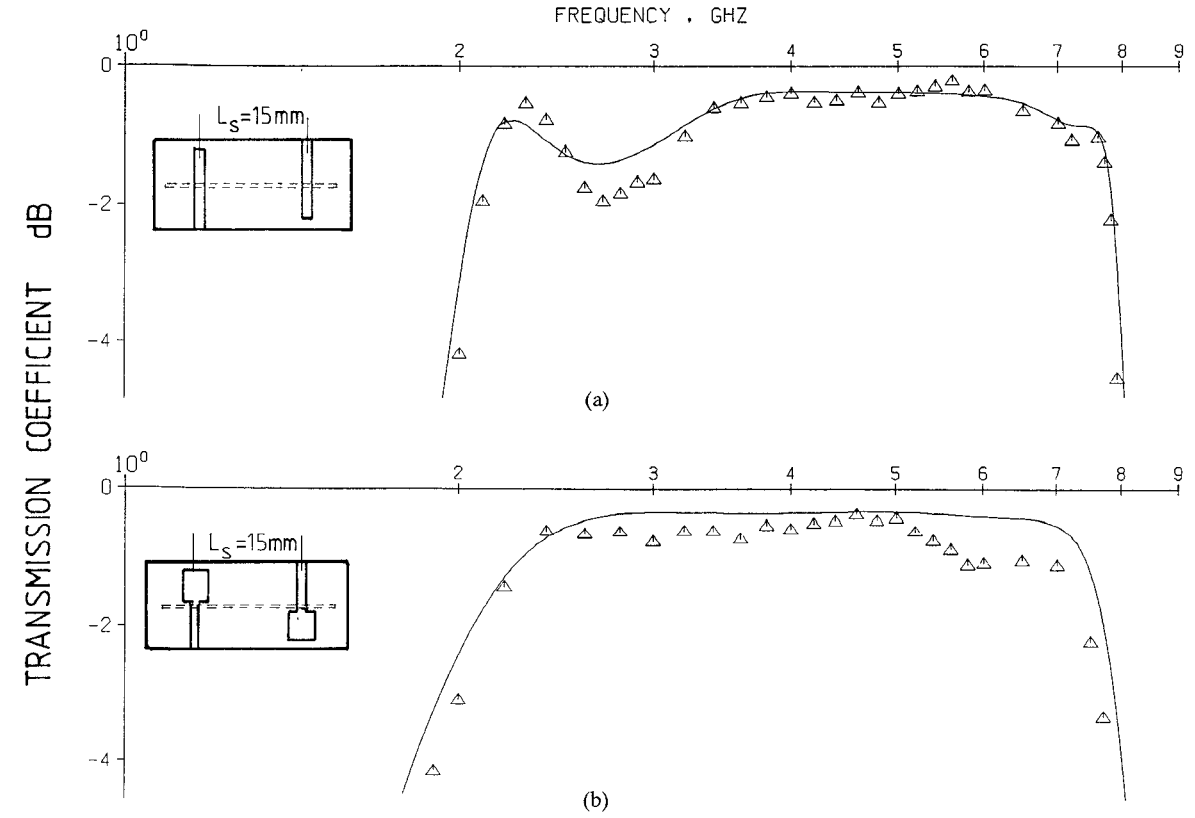

Fig. 10. Transmission coefficient of a cascade of two microstrip/slotline transitions, separated by a slotline of length $L_s = 15$ mm. Theoretical (——) and experimental (△) results. (a) $Z_{mo} = 50\ \Omega$. (b) $Z_{mo} = 19\ \Omega$.

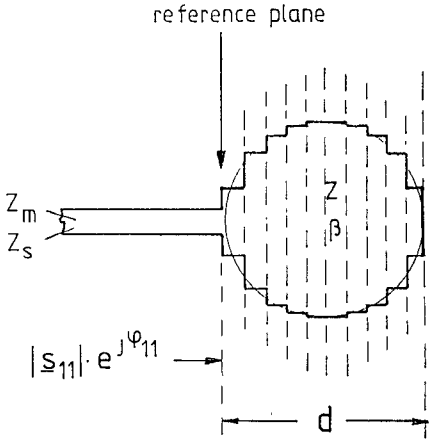

Fig. 11. Basic configuration of a circular stub.

In order to keep the number of figures small, the following results will only be presented for a slotline length of $L_s = 15$ mm. However, calculations and measurements also have been carried out for a slotline length of $L_s = 30$ mm, yielding a quite similar agreement between theory and experiment. The results for a cascade of two transitions with a virtual short using a 50 Ω microstrip stub (see Fig. 6) and a virtual short using a 19 Ω microstrip stub are presented in Fig. 10(a) and (b), respectively. It is recognizable that in both cases the theoretical and experimental results agree surprisingly well; hence the validity of the equivalent circuits and the calculated transition characteristics given in Section III-A has been demonstrated. The good agreement between theory and experiment is surprising, especially in the case of a virtual microstrip short with a 19 Ω stub, because the fringing capacitance of the significant step discontinuity has been neglected.

IV. Broad-Band Transitions

This section is devoted to the analysis and design of broad-band transitions with circular nonuniform lines. For modeling purposes, all nonuniform lines will be treated as tandem-connected segments of piecewise uniform lines, as sketched in Fig. 11. Each nonuniform line is represented by a cascade of 20 line segments of equal length but different characteristic impedances and dispersion characteristics. The validity of such a description has been demonstrated in [10] and [11] for both nonuniform microstrip and slotlines. In this contribution, the end effect of a nonideal microstrip open circuit as well as the end effect of a nonideal slotline short circuit will be neglected.

A. Modeling of a Single Transition

1) Soldered Microstrip Short: Numerical network calculations have been carried out for the circuit of Fig. 2(a) using an equivalent circuit for the circular nonuniform slot stub as given in Fig. 11. The slot stub diameter has been varied between 2.0 and 8.0 mm in steps of 0.5 mm. In the case of the soldered microstrip short, the inductance L_w of the soldered wire has been neglected. The calculated frequency limits against slot stub diameter are given in Fig. 12. Due to the fact that the maximum value of the

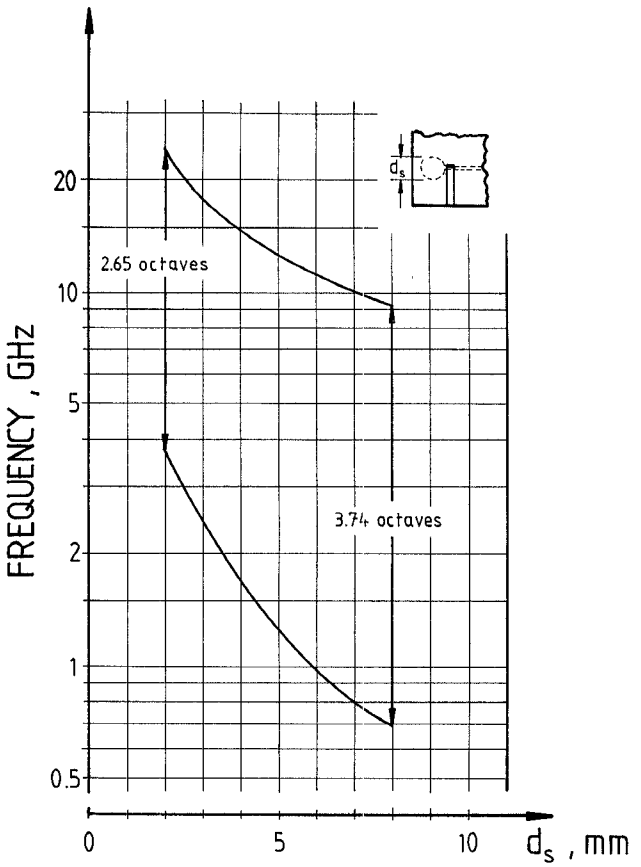

Fig. 12. Calculated −0.97 dB frequency limits against slot stub diameter, for a transition with soldered microstrip short.

characteristic impedance of a circular slot stub increases with increasing slot stub diameter, the achievable bandwidth also increases, whereas the frequency range is shifted towards lower frequencies.

For example, a transition consisting of a soldered microstrip short and a slotline open circuit with a 6 mm diameter offers −0.97 dB band limits of 0.99 GHz and 11.3 GHz, respectively, yielding a bandwidth of 3.5 octaves.

2) Virtual Microstrip Short: If the soldered microstrip short is replaced by a virtual short using a circular nonuniform microstrip line, an equivalent circuit is assumed as given in Fig. 2(b). The circular open microstrip stub and the circular shorted slot stub are again represented by equivalent circuits as given in Fig. 11.

The calculated bandwidth against slot stub diameter of a single microstrip/slotline transition is shown in Fig. 13. The solid line shows the results for a transition with soldered microstrip short for comparison. The dashed lines are valid for a virtual short using different microstrip stub diameters. It is noticeable that the bandwidth of a transition with a virtual short through a circular nonuniform microstrip stub is always lower than the bandwidth of a transition with a soldered microstrip short. However, the bandwidth reduction is rather low, especially for larger slot stub diameters. On the other hand, a virtual short is much easier to fabricate by means of a totally photolithographic technique. Remembering the results of Section II, where

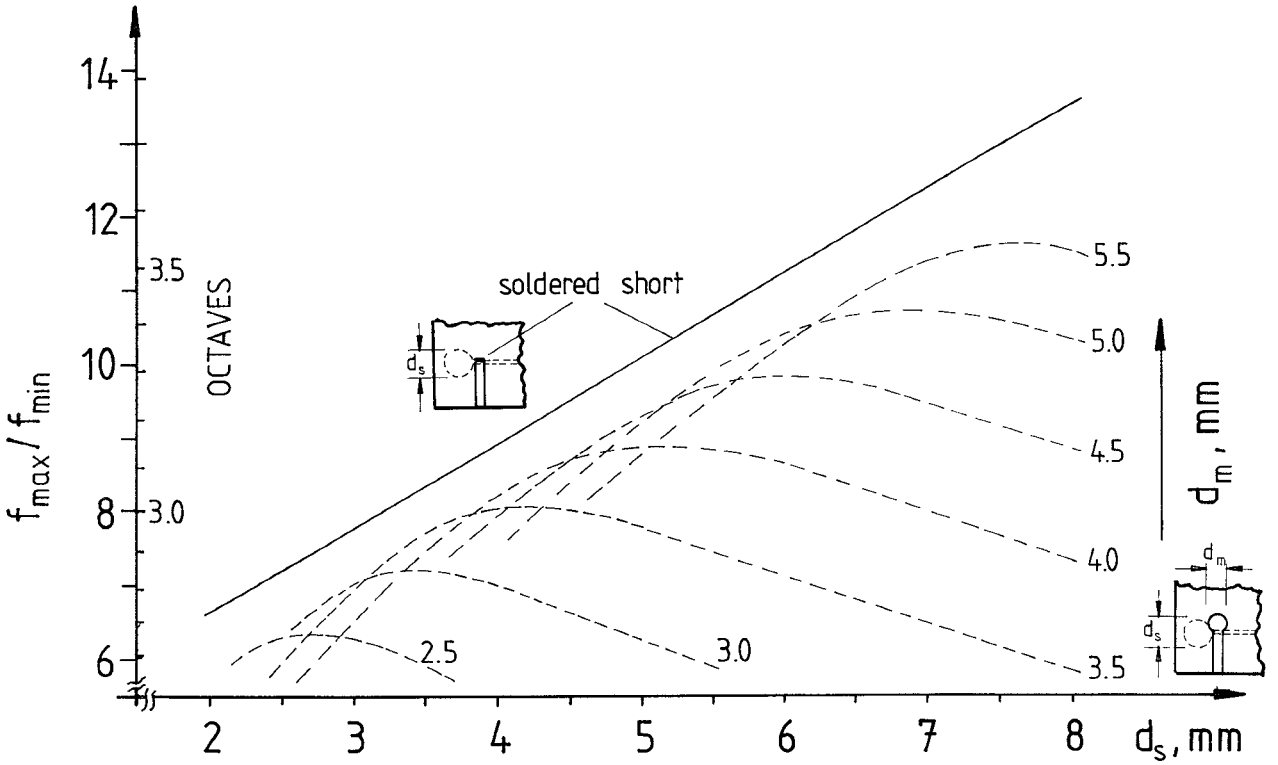

Fig. 13. Bandwidth against slot stub diameter calculated for a single microstrip/slotline transition with *nonuniform* slotline stub. —— soldered microstrip short; ----- virtual microstrip short with different microstrip stub diameters.

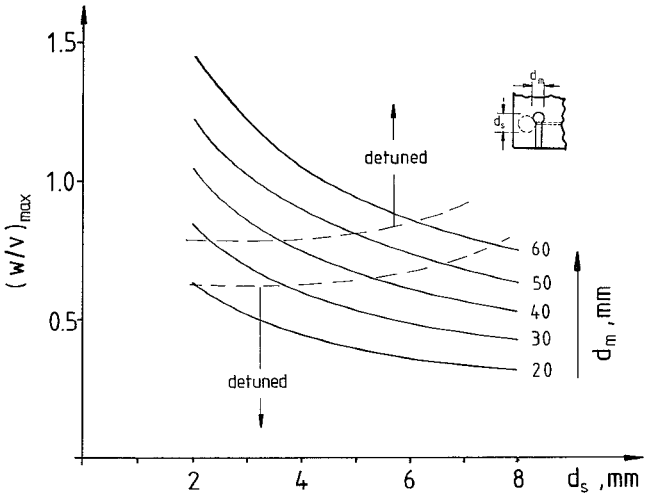

Fig. 14. Impedance relation $(w/v)_{max}$ against slot stub diameter for different microstrip stub diameters.

an improved -0.97 dB bandwidth is predicted in the case of a virtual short if $w > v$, the results of Fig. 13 seem to be contrary to this prediction. To explain this fact, let us consider the relation w/v for different slot stub and microstrip stub diameters, where

$$v_{max} = \frac{Z_{ss_{max}}}{50\ \Omega} \tag{15}$$

$$w_{max} = \frac{50\ \Omega}{Z_{mo_{min}}}. \tag{16}$$

The results are plotted in Fig. 14, where the characteristic impedances in the middle of the stubs have been chosen for comparison. It can be seen that the relation $(w/v)_{max}$ exceeds unity only if both stubs are strongly detuned. This is the case if the electrical lengths of both stubs are too different for a reactance compensating effect. Due to the fact that $w/v < 1$ in the range of interest ($\beta_s l_s \approx \beta_m l_m$), the results of Fig. 13 are absolutely consistent with the basic results of Section II.

The restriction $w/v < 1$ means in practice that the characteristic impedances of a circular microstrip stub cannot be made as low as necessary for a successful bandwidth improvement.

For design purposes it is useful to know optimal combinations of slot stub and microstrip stub diameters. The modeling results for various transitions consisting of different slot stub and microstrip stub diameters are summarized in Fig. 15.

Compared to the -0.97 dB band limits of a soldered transition, the upper and lower band limits are shifted towards lower frequencies if an optimal combination of slot stub and microstrip stub diameter is chosen. The shift of the lower band limiting frequency, which is typically below 100 MHz, is depicted in Fig. 16, whereas the shift of the upper band limiting frequency is typically of the order of a few GHz (Fig. 17).

As an example, let us compare a transition with soldered and virtual short, respectively. For instance, let us consider

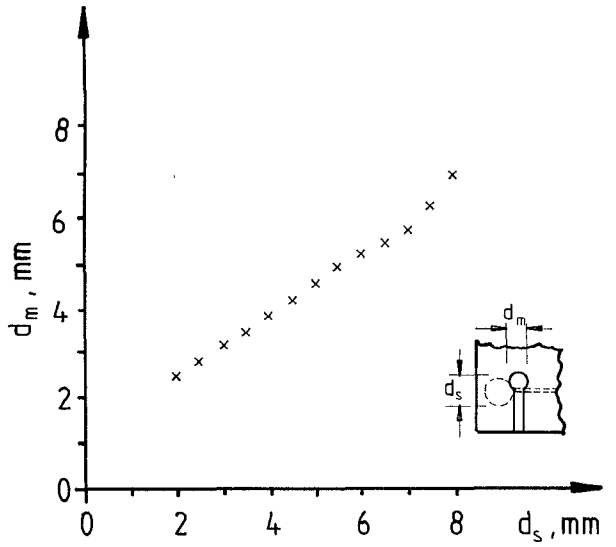

Fig. 15. Optimal microstrip stub diameter against slot stub diameter, modeling results.

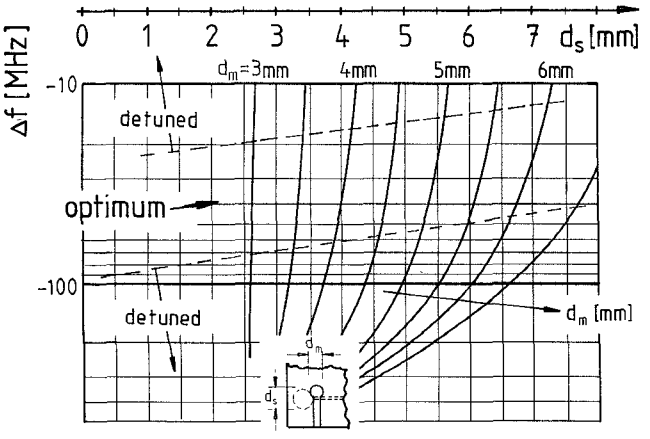

Fig. 16. Calculated frequency shift of the lower −0.97 dB band limits for different microstrip stub diameters, related to the lower band limits of a soldered microstrip–short transition.

a transition with a circular slot stub with a diameter of $d_s = 4.0$ mm.

A transition with a soldered microstrip short has −0.97 dB band limits of 1.65 GHz and 14.91 GHz (Fig. 12), yielding a bandwidth of 3.18 octaves (Fig. 13). In the case of a virtual short with an optimal microstrip stub diameter of $l_m = 4.0$ mm (see Fig. 15), the lower band limit is shifted 45 MHz toward lower frequencies (see Fig. 16), yielding a lower band limiting frequency of about 1.6 GHz. The upper band limit is shifted 1.7 GHz toward lower frequencies (see Fig. 17), yielding an upper band limiting frequency of about 13.2 GHz and a total −0.97 dB bandwidth of 3.04 octaves (Fig. 13).

B. Experimental Verification

As in the case of uniform slotlines and/or microstrip lines (Section III), experimental verification has been carried out by considering a cascade of two transitions sep-

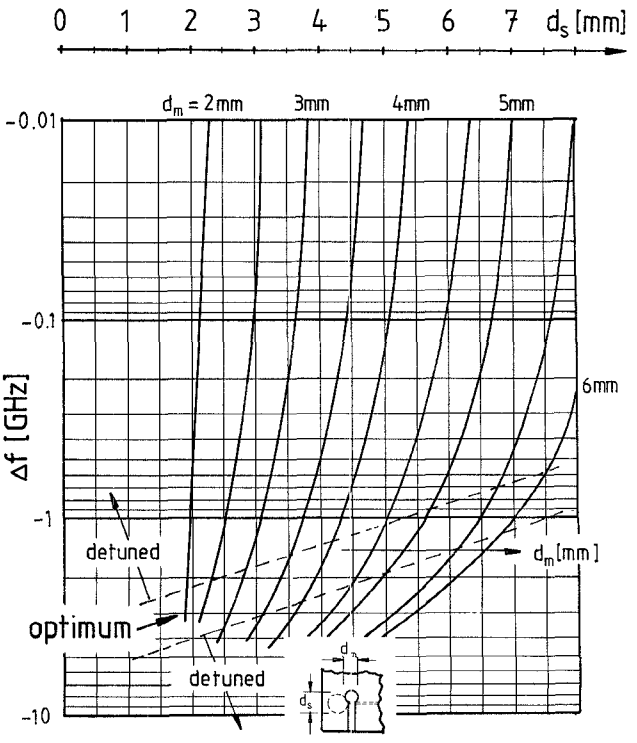

Fig. 17. Calculated frequency shift of the upper −0.97 dB band limits for different microstrip stub diameters, related to the upper band limits of a soldered microstrip–short transition.

arated by a slotline (Fig. 8). Due to the fact that we now deal with transitions which offer a large bandwidth, problems arise from our measurement setup. Even though an automatic network analyzer system was used, it is difficult to achieve reproducible results between microstrip calibration and measurement procedure, especially at frequencies above 12 GHz. Reproducibility problems are mainly due to nonsoldered coax/microstrip transitions. Thus, scattering of measured data points increases with increasing frequency. Moreover, two-port error models for the transitions between coaxial and microstrip line may be too simple to achieve an error-compensated measurement.

The reproducibility of the transmission coefficient if the substrate is removed from the mount and fixed again has been found by measurement to be within 0.8 dB in the frequency range from 12 GHz to 16 GHz, whereas the error is negligible at frequencies below 10 GHz.

The experiments reported here are limited to three different slot stub diameters in conjunction with a soldered microstrip short and one virtual microstrip short, respectively (see Table II). The dimensions (slot and microstrip stub diameters) are chosen in order to realize fixed lower frequency limits of 1, 2, and 4 GHz, respectively. It must be pointed out that these dimensions do not agree with optimal combinations of d_m and d_s referring to Fig. 15 and hence do not offer the maximally achievable bandwidth.

The experimental results together with the modeling results are given in Figs. 18–20. The theoretical and experimental results agree satisfactorily, especially at lower

TABLE II
CALCULATED BANDWIDTH OF SINGLE MICROSTRIP/SLOTLINE TRANSITIONS

Slot Stub Diameter d_s [mm]	Soldered Microstrip Short −0.97 dB band limits (modeling, single transition)	d_m [mm]	Virtual Short −0.97 dB band limits (modeling, single transition)
2.5	2.9 · · · 20.5 GHz	2.0	4.03 · · · 20.5 GHz
5.0	1.26 · · · 12.8 GHz	3.0	2.05 · · · 12.8 GHz
6.0	0.98 · · · 11.3 GHz	5.0	1.02 · · · 10.7 GHz

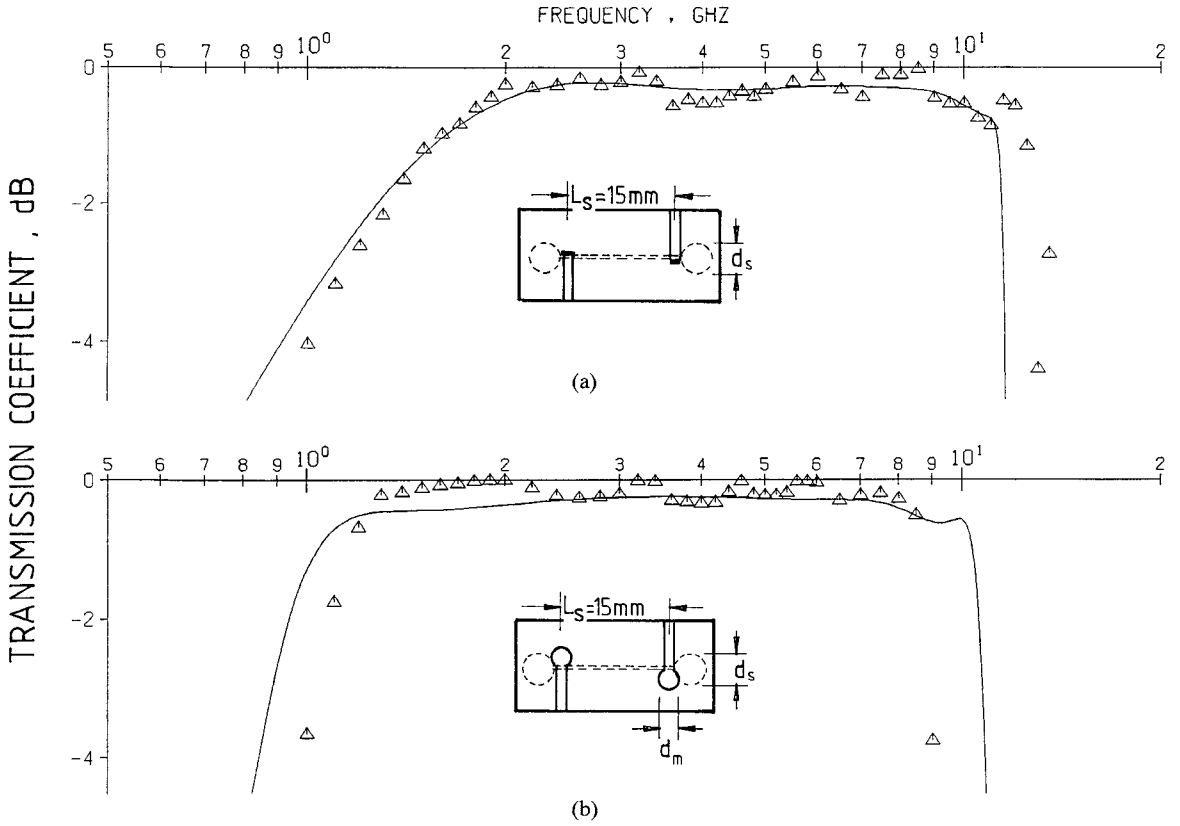

Fig. 18. Fig. 18. Transmission coefficient of a cascade of two microstrip/slotline transitions, separated by a slotline of length $L_s = 15$ mm. Theoretical (——) and experimental (△) results. (a) Microstrip short: soldered; slotline open: circular, $d_s = 6$ mm. (b) Microstrip short: virtual, circular, $d_m = 5$ mm; slotline open: circular, $d_s = 6$ mm.

frequencies. However, in the case of a virtual short, measured behavior different from that of a network model assuming independent lines may occur due to an overlapping of the line shapes of the microstrip and slot stub. This effect tends to increase when dealing with larger stub diameters.

Although this subject is beyond the scope of this work, experiments have been carried out concerning the interaction between microstrip stubs and slot stubs of large diameters. In this case it is advantageous to use a triangular or radial stub [12] instead of a circular stub of the nonuniform microstrip line in order to reduce the overlapping area.

We should remember again that the experimental data as well as the modeling results represent the cascade of two transitions. The bandwidth of a single transition is of course larger than the results of the cascade; the calculated frequency limits of single transitions are given in Table II.

V. CONCLUSIONS

It has been demonstrated that transitions from microstrip to slotline can be described by simple equivalent circuits even when dealing with broad-band transitions incorporating nonuniform lines.

Although a transition with a soldered microstrip short offers the largest bandwidth, optimal combinations of different microstrip and slot stub diameters can be found by modeling. In the case of a virtual short through an optimally chosen circular microstrip stub, the bandwidth is typically about 10 percent below the maximum achievable value of a soldered short.

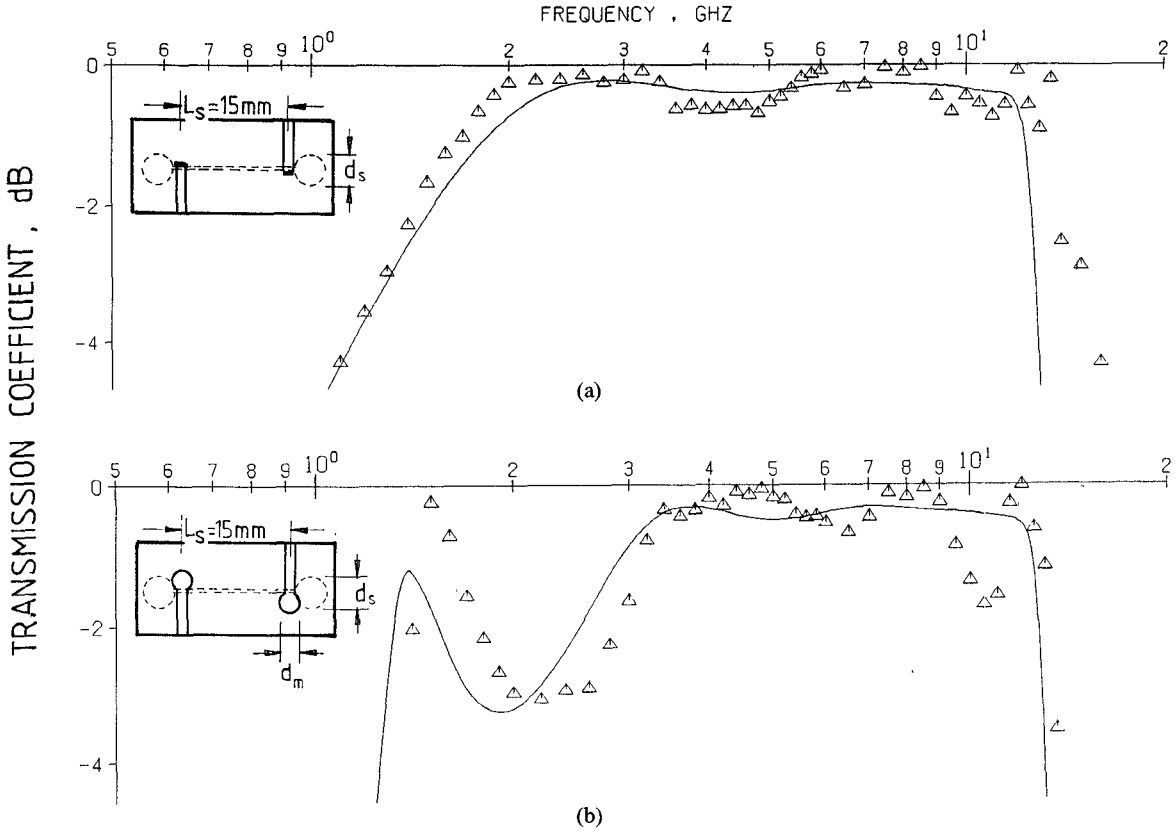

Fig. 19. Transmission coefficient of a cascade of two microstrip/slotline transitions, separated by a slotline of length $L_s = 15$ mm. Theoretical (——) and experimental (△) results. (a) Microstrip short: soldered; slotline open: circular, $d_s = 5$ mm. (b) Microstrip short: virtual, circular, $d_m = 3$ mm; slotline open: circular, $d_s = 5$ mm.

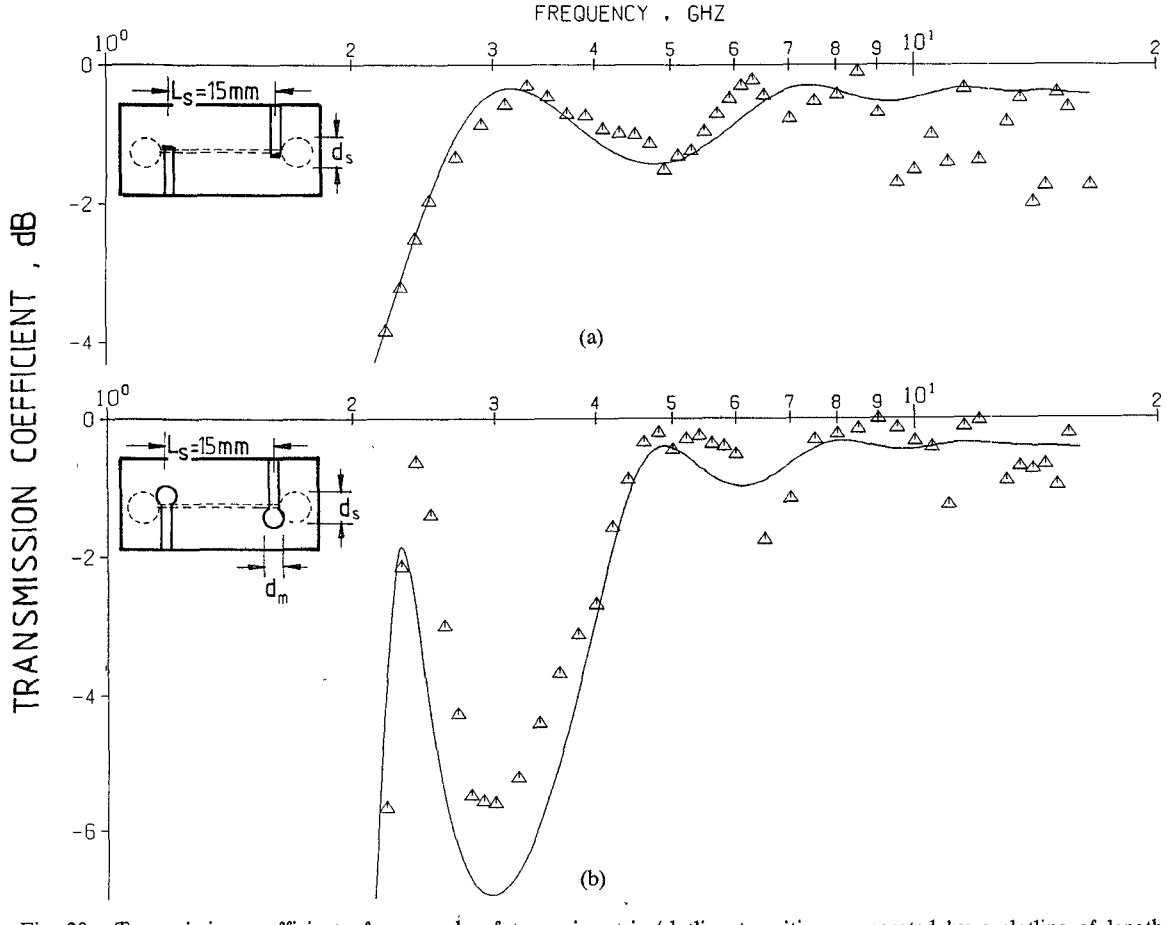

Fig. 20. Transmission coefficient of a cascade of two microstrip/slotline transitions, separated by a slotline of length $L_s = 15$ mm. Theoretical (——) and experimental (△) results. (a) Microstrip short: soldered; slotline open: circular, $d_s = 2.5$ mm. (b) Microstrip short: virtual, circular, $d_m = 2$ mm; slotline open: circular, $d_s = 2.5$ mm.

However, the ease of fabrication of a virtual shorted transition compared to a soldered short is obvious and the small reduction of bandwidth is hence acceptable.

Acknowledgment

Thanks are due to R. Dorra for fabricating some of the MIC's and carrying out some of the measurements and modeling calculations. The author gratefully acknowledges his former colleague G. Böck for discussions and for making available a computer program for calculating the slotline characteristics. He would also like to thank Prof. John for encouragement in studying this subject.

References

[1] S. B. Cohn, "Slot line on a dielectric substrate," *IEEE Trans. Microwave Theory Tech.*, vol. MTT-17, pp. 768–778, 1969.

[2] J. B. Knorr, "Slot-line transitions," *IEEE Trans. Microwave Theory Tech.*, vol. MTT-22, pp. 548–554, 1974.

[3] B. Schiek and J. Köhler, "An improved microstrip to microslot transition," *IEEE Trans. Microwave Theory Tech.*, vol. MTT-24, pp. 231–233, 1976.

[4] F. C. de Ronde, "A new class of microstrip directional couplers," in *Proc. G-MTT-Symp.*, 1970, pp. 184–189.

[5] G. H. Robinson and J. L. Allen, "Slot line application to miniature ferrite devices," *IEEE Trans. Microwave Theory Tech.*, vol. MTT-17, pp. 1097–1101, 1969.

[6] A. Podcameni and M. L. Coimbra, "Slotline-microstrip transition on iso/anisotropic substrate: A more accurate design," *Electron. Lett.*, vol. 16, no. 20, pp. 780–781, 1980.

[7] G. Oltmann, "The compensated balun," *IEEE Trans. Microwave Theory Tech.*, vol. MTT-14, pp. 112–119, 1966.

[8] E. Hammerstad and O. Jensen, "Accurate models for microstrip computer-aided design," in *1980 IEEE MTT-S Int. Microwave Symp. Dig.* (Washington), pp. 407–409.

[9] G. Böck, "Ausbreitungseigenschaften geschichteter, ferritbelasteter Schlitzleitungsstrukturen," Dr.-Ing. thesis, Technische Universität Berlin, Fachbereich 19, 1984.

[10] B. Schüppert, "CAD of nonlinear microwave devices: Development of a balanced mixer having more than 3 octaves bandwidth," in *Proc. 15th European Microwave Conf.*, 1985, pp. 527–532.

[11] B. Schüppert, "Analysis and design of microwave balanced mixers," *IEEE Trans. Microwave Theory Tech.*, vol. MTT-34, pp. 120–128, Jan. 1986.

[12] M. de Lima Coimbra, "A new kind of radial stub and some applications," in *Proc. 14th European Microwave Conf.*, 1984, pp. 516–552.

✠

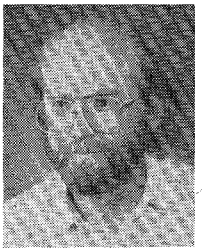

Bernd Schüppert was born on June 5, 1947, in Neunkirchen, West Germany. He received the Dipl.-Ing. degree (1978) and the Dr.-Ing. degree (1983), both in electrical engineering, from the Technische Universität Berlin.

Since 1978, he has been a Research Associate at the Technische Universität Berlin, Institut für Hochfrequenztechnik, working on mixer problems, both theoretically and experimentally. In 1983 and 1984 he worked on a research project on planar balanced broad-band mixers sponsored by the Deutsche Forschungsgemeinschaft. Since 1983, he has been working on Ti:$LiNbO_3$ integrated optic devices as head of the technology group at the Institut für Hochfrequenztechnik.

Dr. Schüppert is a member of the VDE/ITG (Germany).